Materials Letters 240 (2019) 113–116

Contents lists available at ScienceDirect

Materials Letters

journal homepage: www.elsevier.com/locate/mlblue

Toughening mechanisms of epoxy resin using aminated metal-organic framework as additive

Chen Hu [a,b], Juan-Ding Xiao [a,*], Xiao-Dong Mao [a,*], Liang-Liang Song [a], Xin-Yi Yang [a,b], Shao-Jun Liu [a]

[a] Key Laboratory of Neutronics and Radiation Safety, Institute of Nuclear Energy Safety Technology, Chinese Academy of Sciences, Hefei, Anhui 230031, China
[b] University of Science and Technology of China, Hefei, Anhui 230026, China

ARTICLE INFO

Article history:
Received 1 October 2018
Received in revised form 28 November 2018
Accepted 26 December 2018
Available online 4 January 2019

Keywords:
Shielding material
Epoxy resin
Polymers
Mechanical properties
Porous materials
Metal-organic frameworks

ABSTRACT

Improvement of the mechanical properties of epoxy resins (EP), which are used as neutron shielding materials for spent nuclear fuel casks, is becoming very important. In this paper, as representative metal-organic frameworks (MOFs), nanosized UiO-66 and UiO-66-NH_2 were successfully introduced into epoxy resin (EP) by solution casting approach, afford MOF/EP composites, to enhance the mechanical properties. Results clearly showed that MOFs play a vital role in toughening EP-based nanocomposites, and the functioned amino-groups matter the most. Three underlying toughening mechanisms were proposed, which may provide deep understanding of the structure-activity relationship in MOF/polymer composites for radiation shielding application or other academic research.

Nuclear Energy is a promising green power source with attractive development of new nuclear systems such as Generation IV reactor or fusion energy system [1]. The nuclear fuel produced in the nuclear reactor can create a lot of highly radioactive spent nuclear fuel waste, leading to various shielding problems, such as neutron or γ rays shielding [2]. Unwanted exposure to these radiations would be hazardous to human life, which requires a significant demand for developing novel shielding materials in effective protection from different types of radiation [3]. Owing to the abundant hydrogen elements to attenuating fast neutrons, polymer-based composites [4] are interesting candidates for neutron shielding due to their geometric conformability and lighter weight compared with the metal counterparts [5–7], whereas suffer from limitations in mechanical properties for the long-time usage and radiation resistance. To meet this challenge, various micro- or nano-fillers are rationally designed and reinforced into the polymer matrix, and nanomaterials are particular potentials to the strengthened polymer/filler interfacial interaction, which is key to the mechanical properties [8]. However, no systematic study has been carried out to illuminate this structure-mechanical property relationship. Therefore, it is increasingly important to discuss this research field and give a deep insight into structure-mechanical property relationship in polymer-based nanocomposites.

Metal-organic frameworks (MOFs) [9], have recently received considerable attention by virtue of their tunable structures and nanospaces, rich physicochemical properties, as well as potential applications in gas storage and separation, catalysis, sensing, templates, etc [10]. The incorporation of MOF micro- or nano-particles into polymers is an attractable and feasible strategy. The as-formed MOF-based polymer nanocomposite not only combine the high thermal-stability of MOFs and robustness of polymers, but also largely overcome the brittleness and limited mechanical strength of the polymers [11]. The intensive studies toward nano-hybridization of MOFs and polymers thanks to MOFs uniqueness as follows: 1) The inorganic-organic hybrid character of MOFs results in a better compatibility between MOF particles and polymer matrix, which is the key factor for high MOF loading; 2) The porous structure and nano-channels of MOFs facilitate to the regular and controllable polymerization of polymers; 3) The well-defined structures of MOFs are highly desired for studying structure-property relationship in the MOF-based polymer nanocomposite.

In this work, epoxy resin (EP) has been selected as a typical polymer, and two different MOFs, UiO-66/UiO-66-NH_2, have been chosen as the representatives to form UiO-66/EP and UiO-66-NH_2/EP composites, respectively (Fig. S1). UiO-66 and UiO-66-NH_2 nanocrystals were synthesized by hydrothermal method

* Corresponding authors.
E-mail addresses: juanding.xiao@fds.org.cn (J.-D. Xiao), xiaodong.mao@fds.org.cn (X.-D. Mao).

https://doi.org/10.1016/j.matlet.2018.12.123
0167-577X/

according to the reported methods with some modifications [12]. Generally, UiO-66 crystals with an average size around 220 nm and UiO-66-NH_2 about 230 nm were successfully fabricated (Fig. 1a,b and Figs. S2,3). The BET surface areas of UiO-66 and UiO-66-NH_2 are measured to be 1017 and 1004 m^2/g, respectively (Fig. 1c,d). The similar particle sizes and BET surface areas of UiO-66 and UiO-66-NH_2 make it safe to conduct mechanical performance comparison between UiO-66/EP and UiO-66-NH_2/EP, focusing on their difference in the aminated functionality.

The structural integrity of UiO-66 and UiO-66-NH_2 remains very well when introduced into EP matrix according to the powder X-ray diffraction (PXRD) patterns. Detailly, several new peaks (marked with asterisks) appear toward MOF/EP composites, which correspond to PXRD pattern of UiO-66-NH_2 (or UiO-66), indicating MOFs and EP are successfully compounded (Fig. 2a). Additionally, the scanning electron mircroscopy (SEM) observations were shown in Fig. 2b-d. The pure EP have the smooth and glassy surface with no evident plastic deformation, whereas the surface of MOF/EP composites are rather rough, showing MOFs particles are encapsulated within the polymer matrix and uniformly distributed, which is a prerequisite for particle-reinforced polymer matrix.

In order to prove the increased interaction between MOFs and polymer matrix, thermogravimetric analysis was conducted (Fig. S4a and Table S1). Typically, all composites begin decomposing at 250 °C and show double step decomposition regardless of the type of MOFs, and loading of UiO-66 and UiO-66-NH_2 have little influence on thermal properties of the polymers. The glass transition temperatures (T_g) were calculated by the Differential Scanning Calorimeter curves (Fig. S4b). Strikingly, a significant increase in the T_g (129.05 °C) is observed for UiO-66-NH_2/EP composite, which is much higher than that of UiO-66/EP (119.99 °C) and EP (117.32 °C), indicating a stronger interfacial interaction between UiO-66-NH_2 and EP.

Encouraged by the above testing results, the mechanical properties of UiO-66/EP and UiO-66-NH_2/EP composites with same MOF loadings were then investigated. As shown in Fig. 2e, the values of tensile strength and elongation at break for UiO-66-NH_2/EP are 40.4 MPa and 2.60%, respectively, which are higher than that of EP (35.2 MPa and 1.94%) and UiO-66/EP (37.0 MPa and 2.56%). Similarly, UiO-66-NH_2/EP expectedly possesses the highest hardness value of 80.0 compared to that of EP (76.0) and UiO-66/EP (76.6) (Fig. 2f). Furthermore, the fracture surfaces of MOF/EP after exposure to loading are shown in Fig. S5. It is obvious that fillers are embedded in the polymer matrix, proving the strong interfacial interaction and toughening effect of MOFs.

The above results demonstrate that UiO-66-NH_2 has the best influence on the mechanical properties of EP-based composites. To gain further insights into the structure-property relationship, the Fourier Transform infrared spectroscopy (FTIR) measurements were performed (Fig. 3a). The typical peak at ~3400 cm^{-1} is attributed to the hydroxyl and amino group, the corresponding intensity in UiO-66-NH_2/EP is higher than that in EP and UiO-66/EP. It is assumed that the amino groups of UiO-66-NH_2 participate in the reaction and form secondary amine group (N–H) that increase the intensity of FTIR characteristic peak at ~3400 cm^{-1} (Fig. 3b), which results in a better mechanical performance of UiO-66-NH_2/EP composite.

There is additional toughening mechanism proposed from the SEM images of MOF/EP composites (Fig. 3c,d), which can be concluded in the following four parts: 1) Some fillers may be stripped from EP matrix, creating hemi-spherical holes or nanocavities on the fracture surface (toughening mechanism 'A') [13], increasing resistance to the crack propagation. 2) The growth of plastic void (toughening mechanism 'B') around the fillers in some weak regions, releasing the triaxial stress and dissipating the energy [14]. 3) As the horizontal line of the damaged interface rises, the MOF nanoparticles may be partially exposed (toughening mecha-

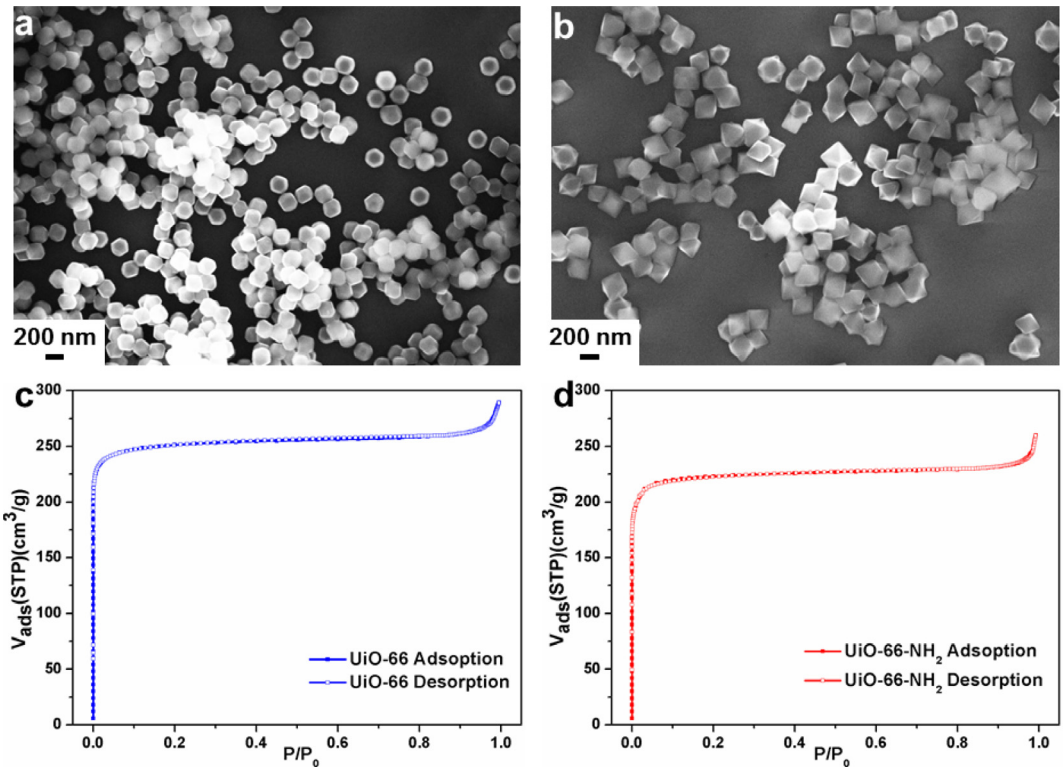

Fig. 1. SEM images and N_2 sorption isotherms at 77 K for (a,c) UiO-66, and (b,d) UiO-66-NH_2.

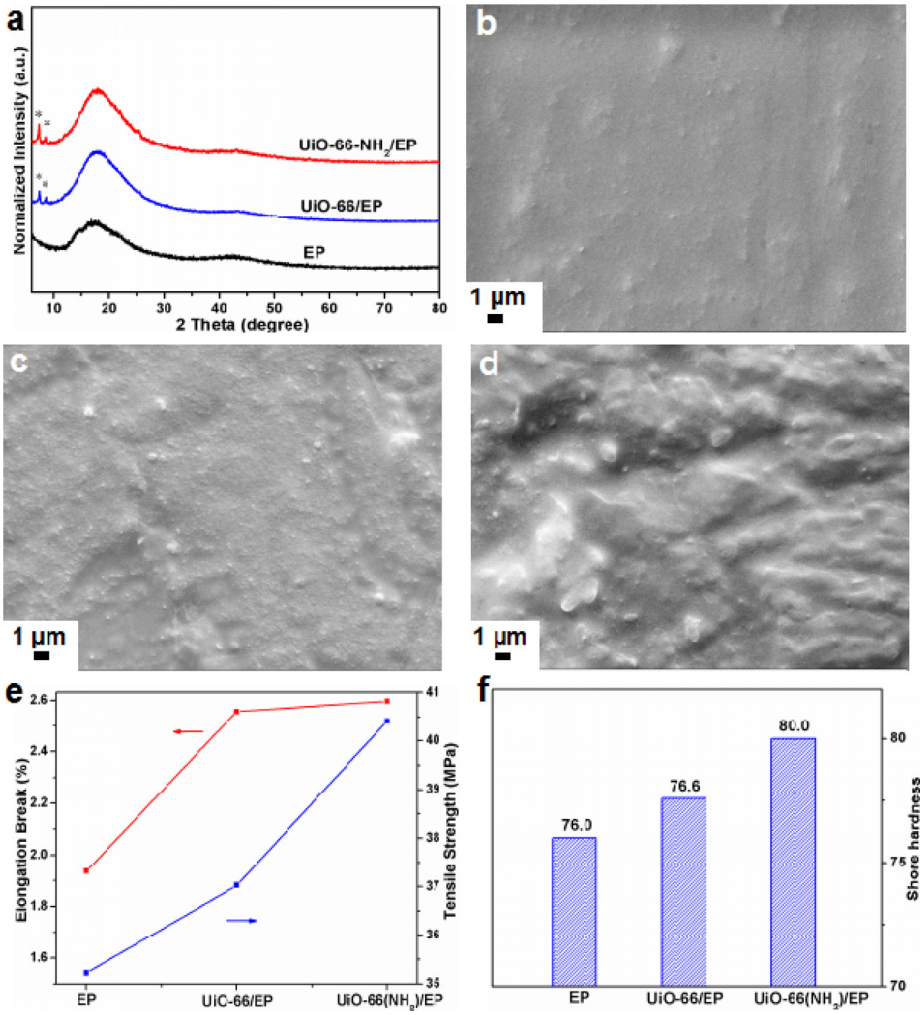

Fig. 2. (a) PXRD patterns, (b-d) SEM images, (e) tensile strength and elongation at break, and (f) shore hardness for neat EP, UiO-66/EP and UiO-66-NH_2/EP, respectively.

nism 'C') or completely covered by the polymer layer (toughening mechanism 'D'), causing cracks to propagate around the poles of MOF particles [15]. 4) When adding exterior stress, the crack propagation is blocked as it approaches the rigid MOFs, leading to the presence of 'tails' hooked behind the particles, which is often recognized as "crack pinning" (toughening mechanism 'E') [16]. In this way, MOF/EP composites would have better mechanical properties than that of the pure EP.

Moreover, it can be observed that the three-dimensional size of the DGEBA monomer is about $1.86 \times 0.85 \times 0.58$ nm (Fig. S6a). UiO-66 and UiO-66-NH_2 have the same topology structures with two different pore sizes of 8 and 11 Å (Fig. S6b) [17]. Therefore, the average pore sizes of the MOFs are large enough to permit DGEBA monomer infiltration and polymerization in the pores, thereby resulting in a unique tight and interpenetrated composite structure [18]. As a result of combined function of these mechanisms, the mechanical properties of the three samples can be ordered as: UiO-66-NH_2/EP > UiO-66/EP > pure EP. Aminated UiO-66-NH_2 with porosity and nanosize characters can inhibit the flaw expansion and protect EP from being pulled off, providing better mechanical properties of UiO-66-NH_2/EP composite than that of pure EP and UiO-66/EP composites.

In summary, MOF/EP composites have been prepared by a facile bulk polymerization strategy. The as-formed UiO-66-NH_2/EP composite displays better mechanical properties than that of EP and UiO-66/EP owing to three toughening mechanisms between UiO-66-NH_2 and EP: 1) amino curing reaction increasing crosslinking degree of EP, 2) the pore structures of UiO-66-NH_2 wrapping polymer chains, and 3) nanosize character of UiO-66-NH_2 enhancing interface interaction. As shown by the ageing results (SI, Section 3, Tables S2, 3), the improved mechanical properties make UiO-66-NH_2/EP more powerful to be utilized in high temperatures. In this way, UiO-66-NH_2/EP is believed to have better radiation resistant ability than the pure EP, and the proposed radiation influence on the polymer-composites has been discussed in SI (Section 4). This paper highlights the amino-functionality, pore structures and nano-size characters of MOFs for enhanced mechanical strength of MOF/polymer composites, and provides technique guidance for deep understanding of the structure-activity relationship in composites.

Declaration of interests

The authors declare that they have no known competing financial interests or personal relationships that could have appeared to influence the work reported in this paper.

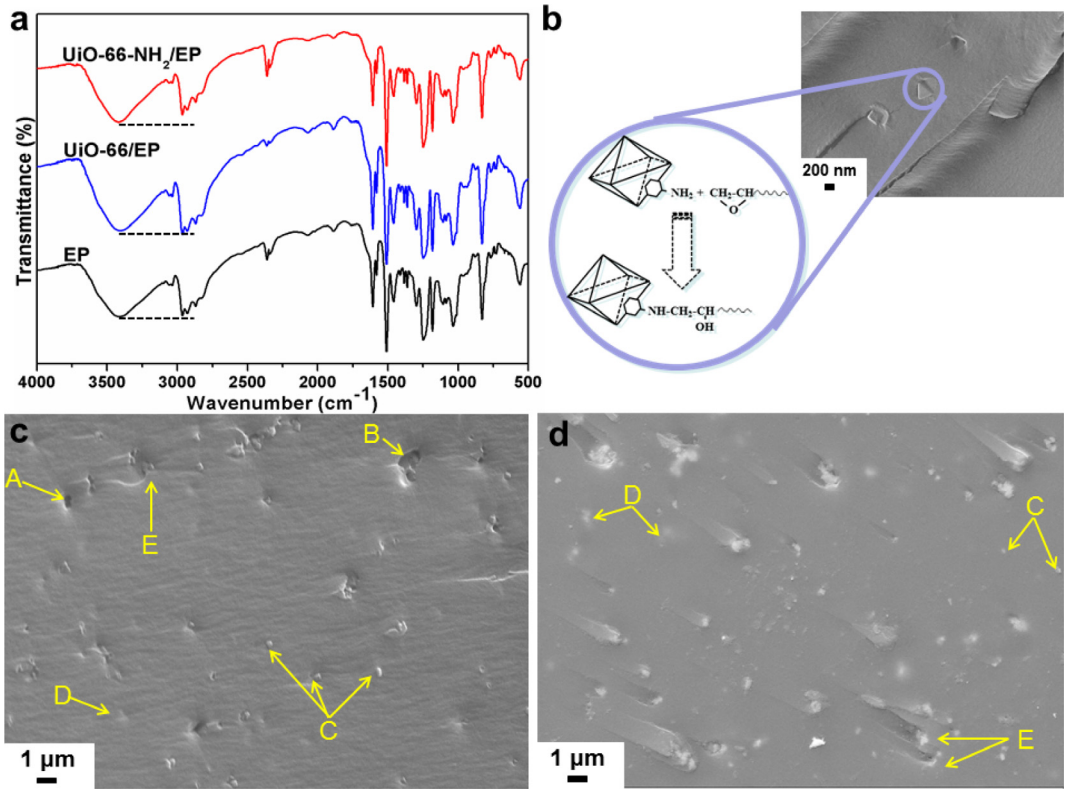

Fig. 3. (a) FTIR spectra. (b) Illustration showing amino groups of UiO-66-NH_2 participated in the reaction. SEM images of fractured surface for (c) UiO-66/EP, and (d) UiO-66-NH_2/EP. Toughening mechanisms are indicated by A, B, C, D and E.

Acknowledgement

This work is supported by the CAS Pioneer Hundred Talents Program, the National Basic Research Program of China with Grant Nos. 2017YFE0300601, and the Provincial Natural Science Foundation of Anhui with Grant Nos. 1704a0902021. The author would like to thank the members in FDS Team for their support and contribution to this research.

Appendix A. Supplementary data

Supplementary data to this article can be found online at https://doi.org/10.1016/j.matlet.2018.12.123.

References

[1] Y. Wu, Y. Bai, Y. Song, Q. Huang, Z. Zhao, L. Hu, Ann. Nucl. Energy 87 (2016) 511–516.
[2] Y. Wu, F.D.S. Team, Fusion Eng. Des. 84 (2009) 1987–1992.
[3] F.A. Cucinotta, M.-H.Y. Kim, L. Ren, Radiat. Meas. 41 (2006) 1173–1185.
[4] S. Nambiar, J.T. Yeow, ACS. Appl. Mater. Inter. 4 (2012) 5717–5726.
[5] Y. Li, Q. Huang, Y. Wu, T. Nagasaka, T. Muroga, J. Nucl. Mater. 367 (2007) 117–121.
[6] Q. Huang, J. Nucl. Mater. 455 (2014) 649–654.
[7] Q. Huang, Nucl. Fusion. 57 (2017) 086042–086050.
[8] N. Lin, J. Huang, A. Dufresne, Nanoscale 4 (2012) 3274–3294.
[9] H.-C. Zhou, J.R. Long, O.M. Yaghi, Chem. Rev. 112 (2012) 673–674.
[10] B. Liu, H. Shioyama, H. Jiang, X. Zhang, Q. Xu, Carbon 48 (2010) 456–463.
[11] Z.P. Smith, J.E. Bachman, T. Li, B. Gludovatz, V.A. Kusuma, T. Xu, D.P. Hopkinson, R.O. Ritchie, J.R. Long, Chem. Mater. 30 (2018) 1484–1495.
[12] M.J. Katz, Z.J. Brown, Y.J. Colón, P.W. Siu, K.A. Scheidt, R.Q. Snurr, J.T. Hupp, O.K. Farha, Chem. Commun. 49 (2013) 9449–9451.
[13] B.B. Johnsen, A.J. Kinloch, A.C. Taylor, Polymer 46 (2005) 7352–7369.
[14] A.G. Evans, S. Williams, P.W.R. Beaumont, J. Mater. Sci. 20 (1985) 3668–3674.
[15] D. Hull, Fractography: Observing, measuring, and interpreting fracture surface topography, Cambridge University, Cambridge, 1999.
[16] B.B. Johnsen, A.J. Kinloch, R.D. Mohammed, A.C. Taylor, S. Sprenger, Polymer 48 (2007) 530–541.
[17] N.A. Ramsahye, J. Gao, H. Jobic, P.L. Llewellyn, Q. Yang, A.D. Wiersum, M.M. Koza, V. Guillerm, C. Serre, C.L. Zhong, G. Maurin, J. Phys. Chem. C 118 (2014) 27470–27482.
[18] X. Yang, X. Jiang, Y. Huang, Z. Guo, L. Shao, ACS. Appl. Mater. Interfaces 9 (2017) 5590–5599.